Caving 2022 - Y Potvin (ed.)

doi:10.36487/ACG_repo/2205_32

Quantitative correlation of production and seismic response in block caves

W de Beer *ESG Solutions Pty Ltd, Australia*

Abstract

Rates and sequencing of undercut production blasting, drawbell blasting, and mucking are key drivers of cave performance. Cave performance encompasses a range of factors, which include growth, shape and the effect of the cave on the abutments, excavations, geological structures and lithology. We calculate Spearman's rank correlation coefficient for time series of the seismic response in work areas, around geological structures, and in geotechnical domains in a block cave. These comparisons enable quantification of the relationship between production rates and seismic response.

Keywords: *production, seismicity, correlation*

1 Introduction

When mining occurs there often is a seismic response. The size and the time of the response differ from mine to mine and even from place to place in a mine, and there are interactions between different parts of the rock mass system (lithological units, geotechnical domains, structures, pillars, and excavations).

Mining perturbs an in situ stress equilibrium by creating excavations underground and/or large holes on surface (Gibowicz & Kijko 1994). In either case, stress is transferred into the surrounding rock mass. In underground mining the transferred stress can increase the ambient stress to exceed intact rock strength. Close to excavations, where the nearby free surface allows movement, it can exceed the frictional clamping on faults, leading to fault slip, or it can cause slipping or buckling in or near stiffness contrasts (e.g. between strong brittle intrusives and other softer lithologies.). In turn stress release on structures (when a structure becomes active) or near an excavation (e.g. a rockburst or pillar burst) can transfer stress to other locations. Any of these situations can lead to sudden inelastic deformation – a seismic event.

Techniques to understand the effect of production rates on seismicity in space and time, and the relationships between seismic response in different parts of the mine include the concept of volume of ground mined (McGarr 1976), modelling and time links (Kaiser et al. 2005). Naïve application of these techniques risk falling prey to the post hoc ergo propter hoc fallacy (because a rooster always crows before the dawn, the crowing rooster causes the dawn), while others may be prone to a proximity fallacy (just because a seismic event locates close to a fault does not mean that the event is fault slip). We do not claim that the statistical technique illustrated here is free of fallacies (it is prone in particular to confusing correlation and causation) but we illustrate it as a quantitative method to aid avoiding against the fallacies above. Calculation of Spearman correlations (Clarke & Cooke 1978) are computationally relatively cheap and could be used to rapidly test assumptions about apparent related activity.

We use potency P in this paper, where potency tensor is given by the integral of the strain rate over the duration and volume of the source (Ben-Zion & Lyakhovsky 2019). The scalar seismic moment, $M_o = \mu P$ (in N·m), where μ is the shear modulus of the rock. By 'mining' we mean here production (undercut ring) blasting, drawbell blasting, and mucking. We use the language of stress transfer, but we are aware of formulations that consider deformation transfer. Our interest is in ways of visualising and quantifying interactions, whichever way the interaction between different locations and drivers are mediated. The question addressed in this paper is whether there are quantifiable correlations between production rates and seismic response.

2 Methodology

Seismogenic zones are initially delineated by eye and then refined by using a density based spatial clustering with noise (DBSCAN) algorithm based on locations. This serves as a guide to defining the target areas to be studied (Figure 1). Zones are often divided into volumes above, and in and below the undercut to probe the expected different responses between these areas (events above the undercut are expected to be associated with caving or the propagation of the seismogenic zone; those below with stress and strain energy accumulation in pillars). To consider the relationship between seismic response and production in different panels, a moving spatial window is used. The window size is four panels, and the step size is one panel (i.e. we consider production in, say, panels 5–8, 6–9, 7–10, …).

Time series of cumulative seismic potency ($\Omega = \sum P$, essentially $\sum M_o$), and production (cumulative production blasts, $V_{GM(P)} = \sum A_R$, where A_R is the area of the rings blasted (usually given in m^2), cumulative drawbell blasting $V_{GM(DP)} = \sum C_{DB}$, where C_{DB} is the charge used or number of rings, and cumulative mucking $V_{GM(M)} = \sum M_{DP}$ where M_{DP} is tons of material mucked at a drawpoint (Figure 2) are constructed and analysed qualitatively as well as quantitatively by examining them for correlations using the Spearman's rank correlation coefficient (Clarke & Cooke 1978).

Spearman's rank correlation coefficient (r_S) provides an estimate of how monotonic the relationship is between two variables. It requires pairs of data at regular intervals, so we sample the cumulative series at intervals Δt = 24h, 48h, 72h and 96h. The sampled production/response time series pairs are regularised by setting their start times to the earliest of the two, and the end times to the latest of the two.

Since cumulative variables are considered, a high r_S is to be expected and does not convey much information. Of more interest is r_S for the rates of change and the direction of the change of these derivative quantities. Therefore, we construct time series of the first ($\dot{\Omega} = \Delta\Omega/\Delta t$, $\dot{V}_{GM(P)} = \Delta V_{GM(P)}/\Delta t$, $\dot{V}_{GM(DP)} = \Delta V_{GM(DP)}/\Delta t$, $\dot{V}_{GM(M)} = \Delta V_{GM(M)}/\Delta t$) and second order rates of change ($\ddot{\Omega}$, $\ddot{V}_{GM(DP)}$, $\ddot{V}_{GM(M)}$) for Δt = 24h, 48h, 72h and 96h. The coefficient r_S is calculated for lag times $t_{Lag} = n \cdot \Delta t$, $n = 0, 1, 2$ and 4 between the seismic response and the production (i.e. the correlation between the production at time (t) and the seismic response at $t + n\Delta t$.

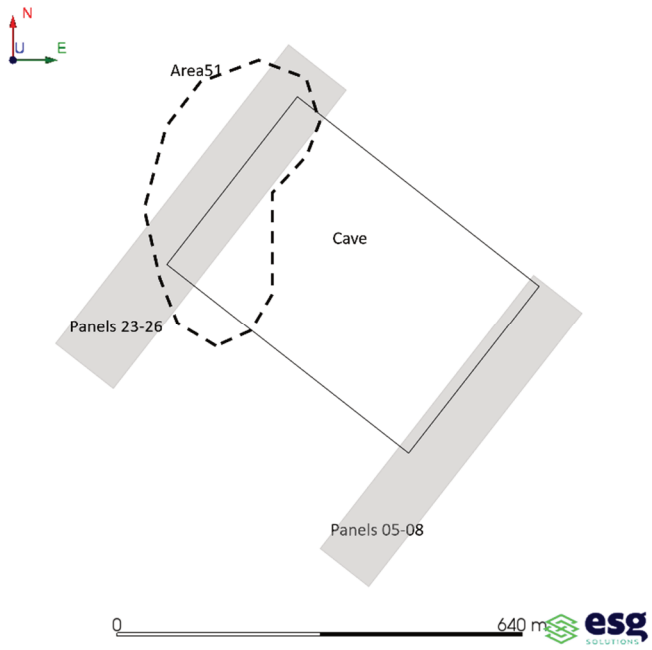

Figure 1 Seismogenic zone Area51, production panels 23–26 and 05–08

3 Data

Production data comprises ring blasts (in square metre per ring), drawbell blasting (nominally given in terms of the mass of the charge), and mucking (tons). A considerable amount of work is required to format the data into a form amenable to comparison with seismic data. The key problem is to geolocate the blasts and drawpoints and assign times to them. Partly for this reason, and partly because the formalism require regularly sampled time series, daily totals are used.

Seismic data are sourced from the ESG SQL real-time database for the mine. Standard practice is to use data spanning three months but here we consider data from over a 10-month period. At this stage, we used all events (we did not apply a magnitude of completion cut-off).

Figures 2 to 4 show the one-day sampled, regularised cumulative potency and cumulative production variables plotted on one graph for Area51, the area of interest here.

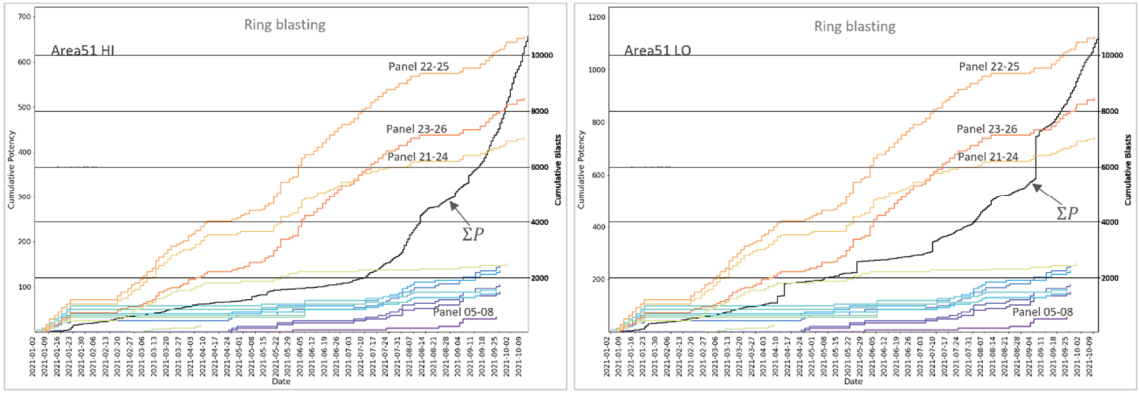

(a) (b)

Figure 2 Cumulative seismic potency (black line) in the Area51 zone, (a) above, and (b) in and below the undercut, plotted with production blasting (coloured lines) in panels

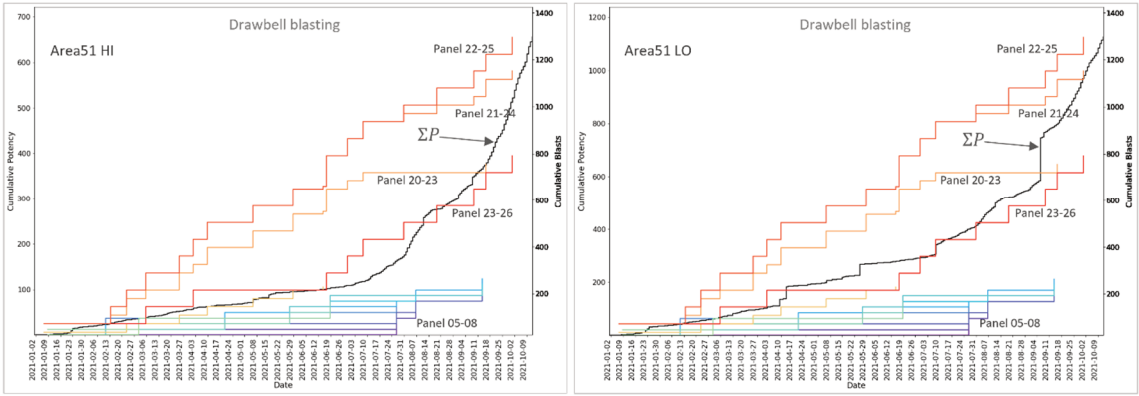

(a) (b)

Figure 3 Cumulative seismic potency (black line) in the Area51 zone, (a) above, and (b) in and below the undercut, plotted with drawbell blasting (coloured lines) in panels

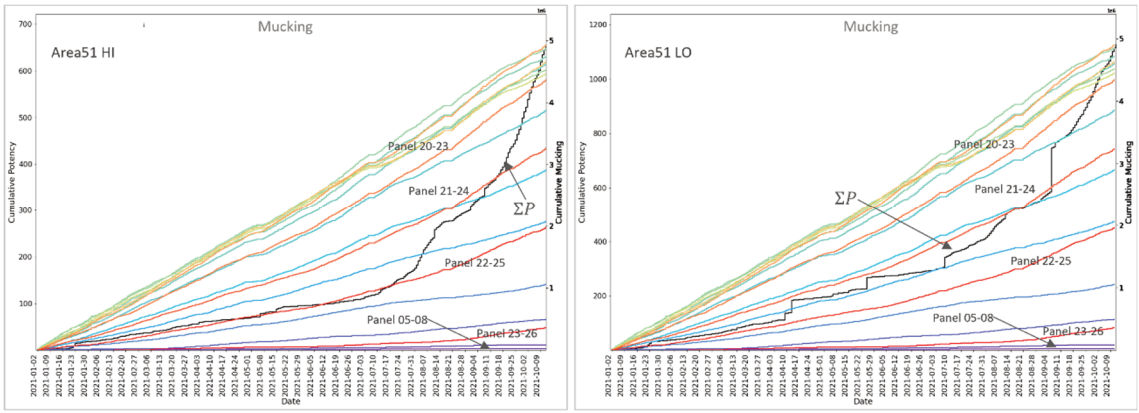

(a) (b)

Figure 4 Cumulative seismic potency (black line) in the Area51 zone, (a) above, and (b) in and below the undercut, plotted with mucking (coloured lines) in panels

4 Results

In what follows, we show only the sampling period/lag time combinations which produced the highest values of r_S.

4.1 Zero order: cumulative quantities

The Spearman correlation coefficient calculated for cumulative potency in Area51 and production blasting (Figures 5 and 6, in and below, and above the undercut, respectively), drawbell blasting (Figures 7 and 8) and mucking (Figures 9 and 10) shows a generally strong positive rank-based correlation. This is not surprising, as r_S indicates the strength of monotonicity and cumulative quantities can only increase or stay the same. The zero values in Figures 5 to 10 are because there was no production activity of that type in the relevant panels in the time window under consideration. Lower values show the effect in the multi-panel production areas of such areas.

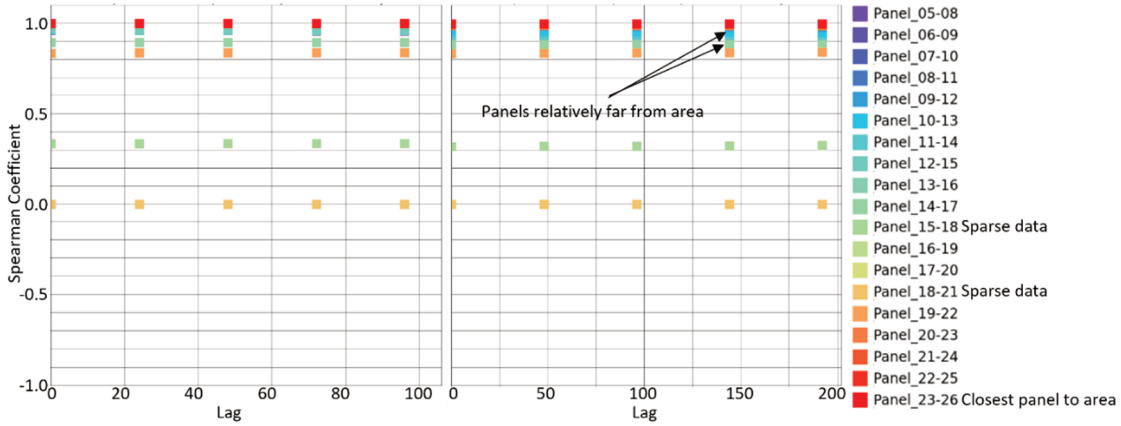

Figure 5 Spearman correlation coefficient calculated for cumulative potency in Area51, in and below the undercut, and cumulative production blasting for time series sampled at equal time intervals Δt = 24h and 48h (left, right) and lag times $t_{Lag} = n \cdot \Delta t, n$ = 0, 1, 2, 3 and 4

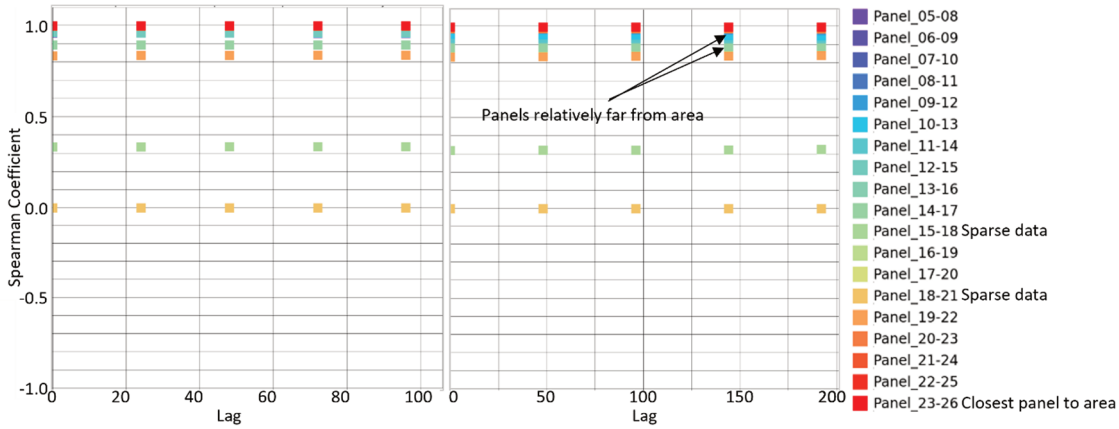

Figure 6 **Spearman correlation coefficient calculated for cumulative potency in Area51, above the undercut, and cumulative production blasting for time series sampled at equal time intervals Δt = 24h and 48h (left, right) and lag times $t_{Lag} = n \cdot \Delta t, n$ = 0, 1, 2, 3 and 4**

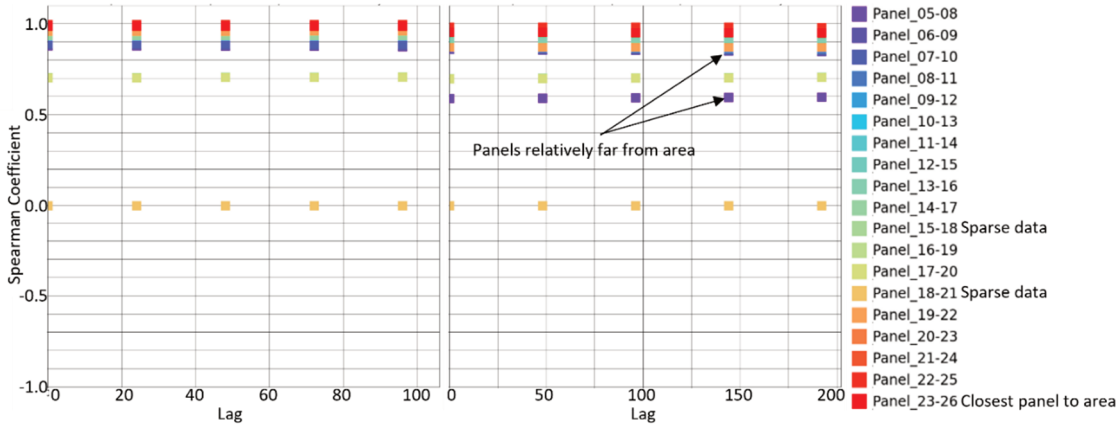

Figure 7 **Spearman correlation coefficient calculated for cumulative potency in Area51, in and below the undercut, and cumulative drawbell blasting for time series sampled at equal time intervals Δt = 24h and 48h (left, right) and lag times $t_{Lag} = n \cdot \Delta t, n$ = 0, 1, 2, 3 and 4**

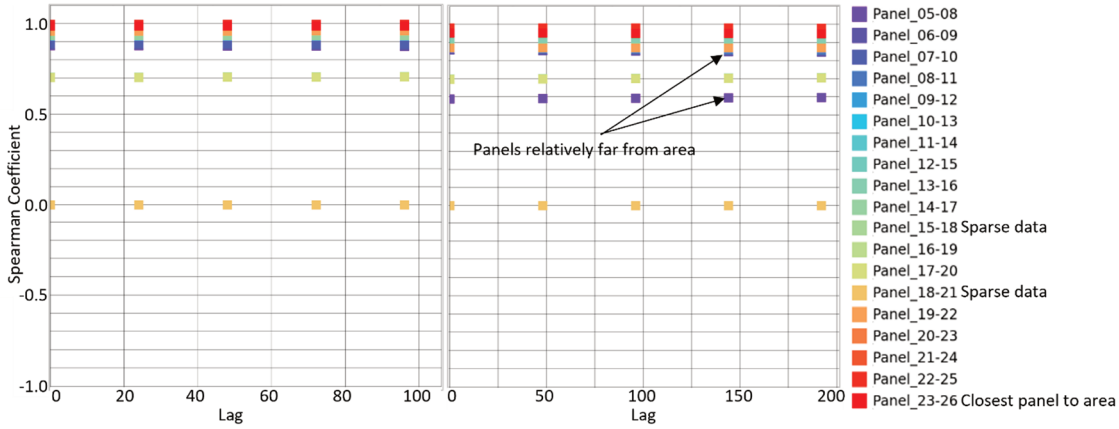

Figure 8 **Spearman correlation coefficient calculated for cumulative potency in Area51, above the undercut, and cumulative drawbell blasting for time series sampled at equal time intervals Δt = 24h and 48h (left, right) and lag times $t_{Lag} = n \cdot \Delta t, n$ = 0, 1, 2, 3 and 4**

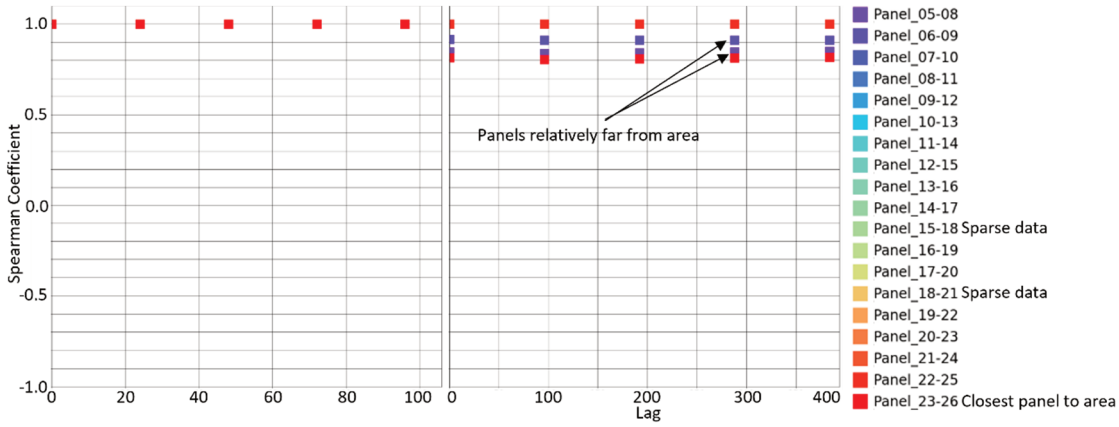

Figure 9 Spearman correlation coefficient calculated for cumulative potency in Area51, in and below the undercut, and cumulative mucking for time series sampled at equal time intervals Δt = 24h and 96h (left, right) and lag times $t_{Lag} = n \cdot \Delta t, n$ = 0, 1, 2, 3 and 4

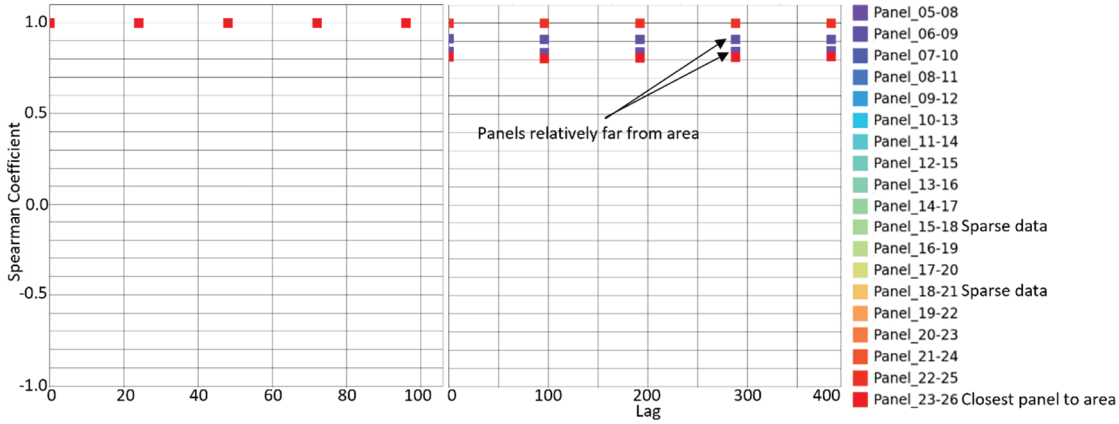

Figure 10 Spearman correlation coefficient calculated for cumulative potency in Area51, above the undercut, and cumulative mucking for time series sampled at equal time intervals Δt = 24h and 96h (left, right) and lag times $t_{Lag} = n \cdot \Delta t, n$ = 0, 1, 2, 3 and 4

4.2 First order: slopes of cumulative quantities

For the production blasting (Figures 11 and 12), the largest positive correlation for change in the quantities is for the easternmost panels 05 to 08. If the slopes $\dot{\Omega} = \Delta\Omega/\Delta t$, $\dot{V}_{GM(P)} = \Delta V_{GM(P)}/\Delta t$, for the seismic potency and the production blasts, respectively, are calculated over Δt = 48h or 96h, and the resultant values $\dot{\Omega}(t)$ and $\dot{V}_{GM(P)}(t - 96h)$ compared, the largest r_S is obtained. Correlations for panels further from the seismic zone (lower panel numbers) are also more positive. This is an example of the fact that correlation is not causation: it is serendipitous that blasting occurred in the eastern panels (lower numbers) at the same time as the seismic response changed in the west (higher numbers). At this stage the cave was relatively mature, so the likelihood of stress transfer from the eastern to the western side was small. On the other hand, the correlation between western panels and the western seismogenic zone is more strongly suggestive of a causal relationship. The correlation with drawbell blasting is generally weak (Figures 13 and 14), while mucking shows strong correlations (Figures 15 and 16) for the panels closest to or in the seismogenic zone. There are again high correlations with some more distant panels. Again, these correlations could be accidental. We will from now on ignore the distant panels (see comment above about maturity of the cave).

Correlation weakens and essentially disappears as the calculation of the rate of change is performed over larger intervals. Using a shorter interval captures fast, high frequency changes while the longer intervals measure long-term, average rates of change.

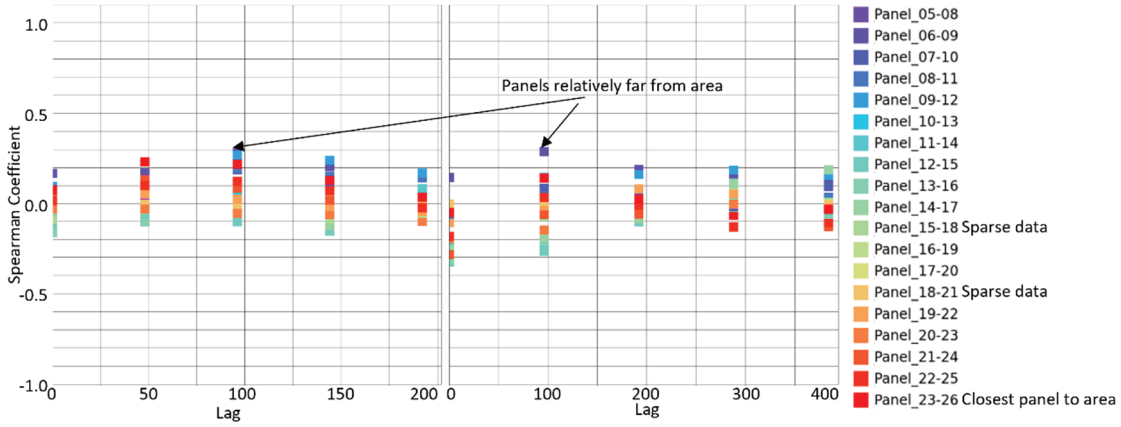

Figure 11 Spearman correlation coefficient calculated for the slopes of the cumulative potency in Area51, in and below the undercut, and the cumulative production blasting for time series sampled at equal time intervals Δt = 48h and 96h (left, right) and lag times $t_{Lag} = n \cdot \Delta t, n$ = 0, 1, 2, 3 and 4

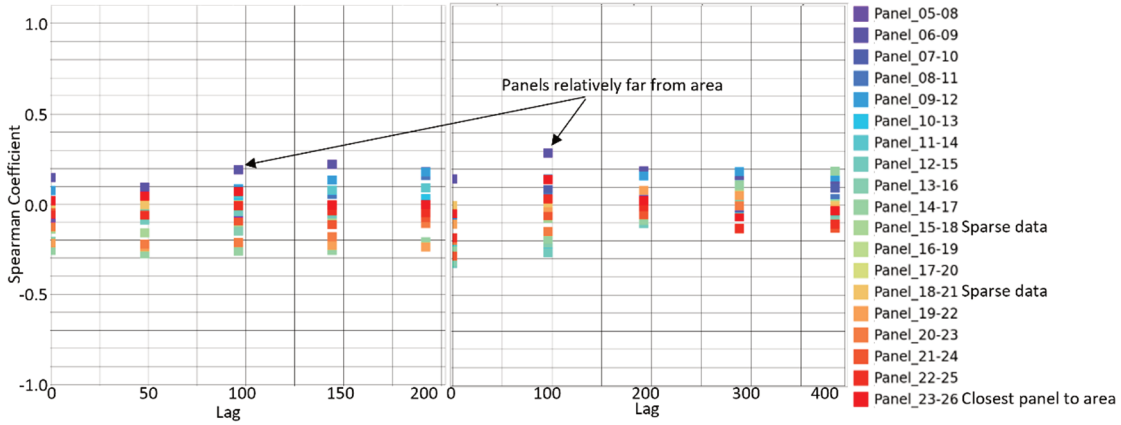

Figure 12 Spearman correlation coefficient calculated for the slopes of the cumulative potency in Area51, above the undercut, and the cumulative production blasting for time series sampled at equal time intervals Δt = 48h and 96h (left, right) and lag times $t_{Lag} = n \cdot \Delta t, n$ = 0, 1, 2, 3 and 4

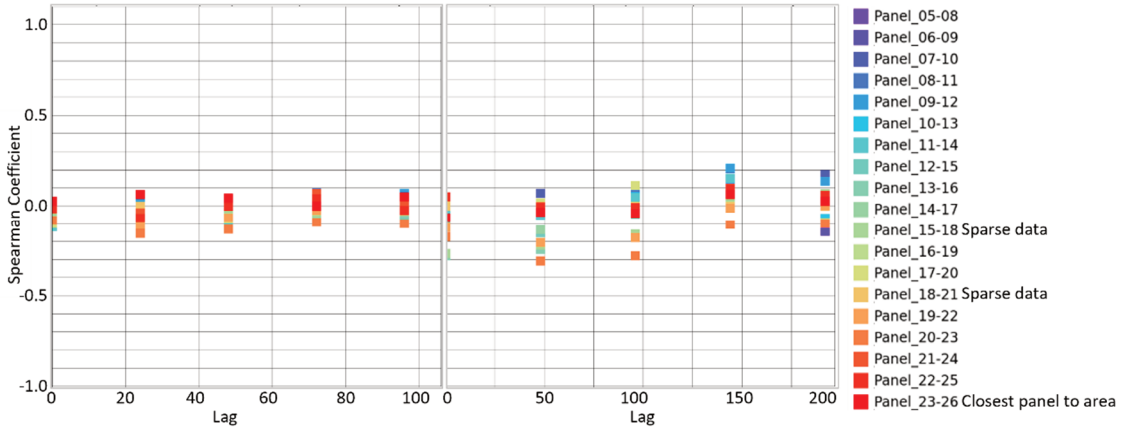

Figure 13 Spearman correlation coefficient calculated for the slopes of the cumulative potency in Area51, in and below the undercut, and the cumulative drawbell blasting for time series sampled at equal time intervals Δt = 24h and 96h (left, right) and lag times $t_{Lag} = n \cdot \Delta t, n$ = 0, 1, 2, 3 and 4

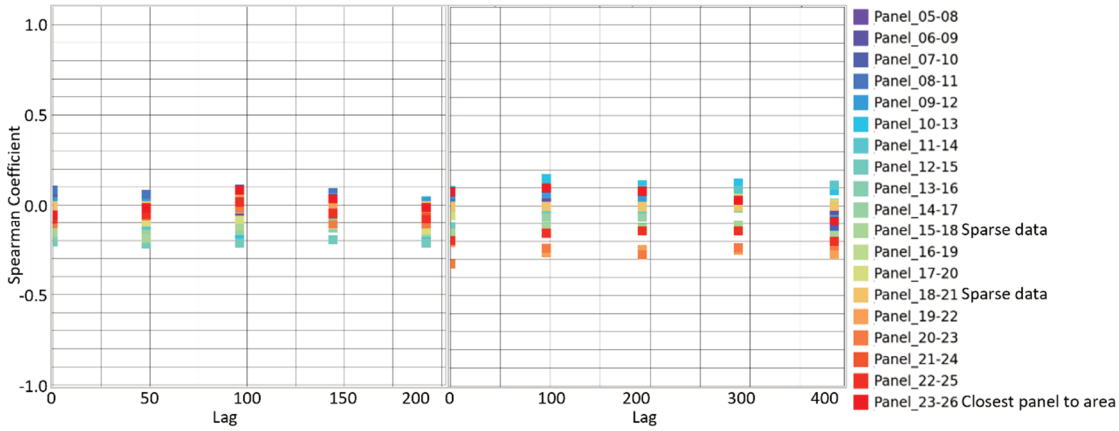

Figure 14 Spearman correlation coefficient calculated for the slopes of the cumulative potency in Area51, above the undercut, and the cumulative drawbell blasting for time series sampled at equal time intervals Δt = 28h and 96h (left, right) and lag times $t_{Lag} = n \cdot \Delta t, n$ = 0, 1, 2, 3 and 4

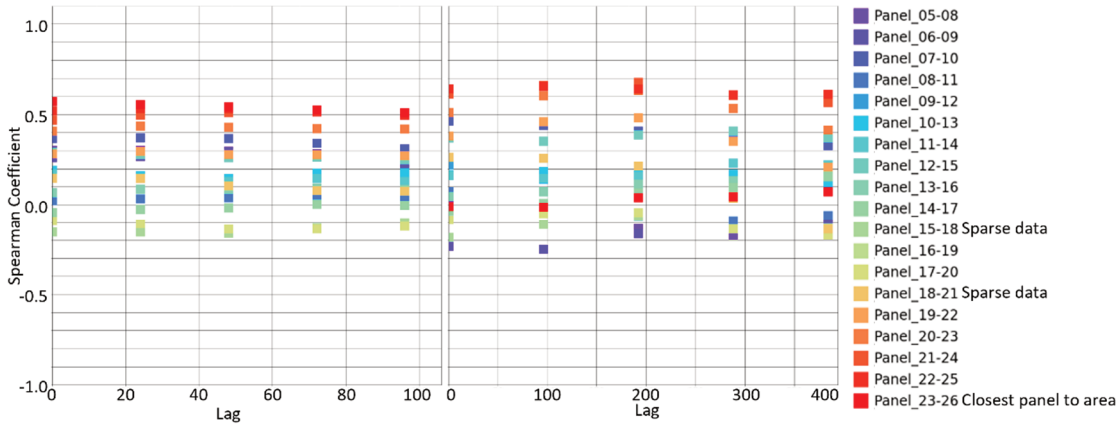

Figure 15 Spearman correlation coefficient calculated for the slopes of the cumulative potency in Area51, in and below the undercut, and the cumulative mucking for time series sampled at equal time intervals Δt = 24h and 96h (left, right) and lag times $t_{Lag} = n \cdot \Delta t, n$ = 0, 1, 2, 3 and 4

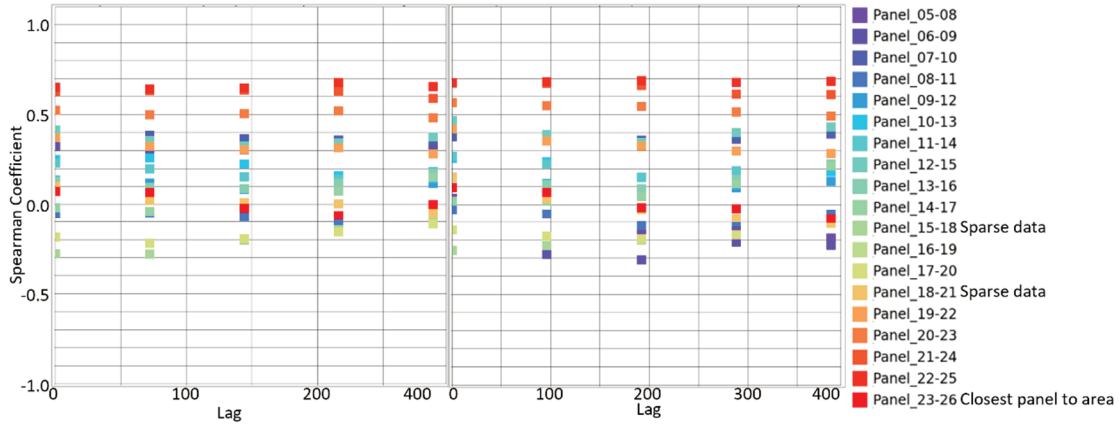

Figure 16 Spearman correlation coefficient calculated for the slopes of the cumulative potency in Area51, above the undercut, and the cumulative mucking for time series sampled at equal time intervals Δt = 72h and 96h (left, right) and lag times $t_{Lag} = n \cdot \Delta t, n$ = 0, 1, 2, 3 and 4

4.3 Second order: rate of change of slopes of cumulative quantities

The accelerations in seismic response in the Area51 zone in and under the undercut and production blasting (Figures 17 and 18) show moderate correlations for the panels closest to or inside the seismogenic zone, like the rate of change correlations. The correlation with drawbell blasting and mucking is generally moderate (Figures 19 and 20, and Figures 21 and 22, respectively). There are again counterintuitive cases of high r_S values associated with seismic volumes and production in distant panels. Again these will be ignored going forward.

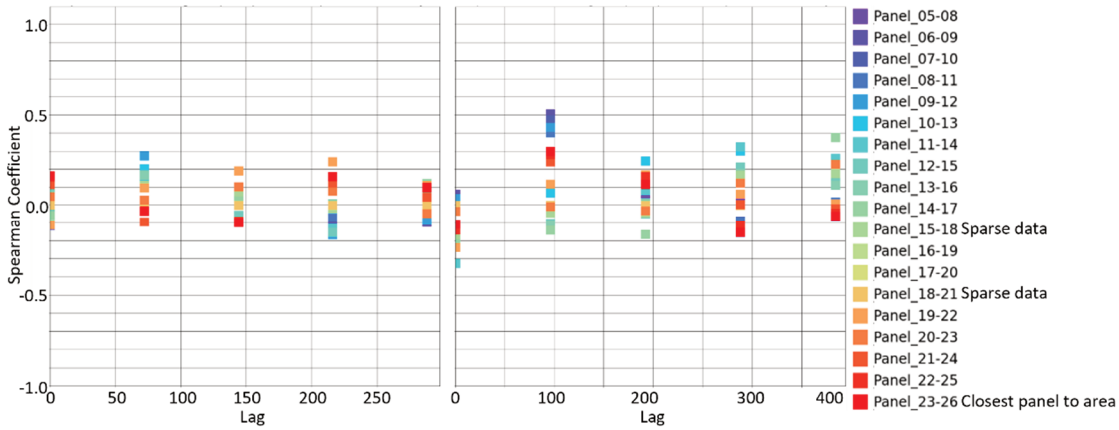

Figure 17 Spearman correlation coefficient calculated for the rate of change of the slopes of the cumulative potency in Area51, in and below the undercut, and the cumulative production blasting for time series sampled at equal time intervals Δt = 72h and 96h (left, right) and lag times $t_{Lag} = n \cdot \Delta t, n$ = 0, 1, 2, 3 and 4

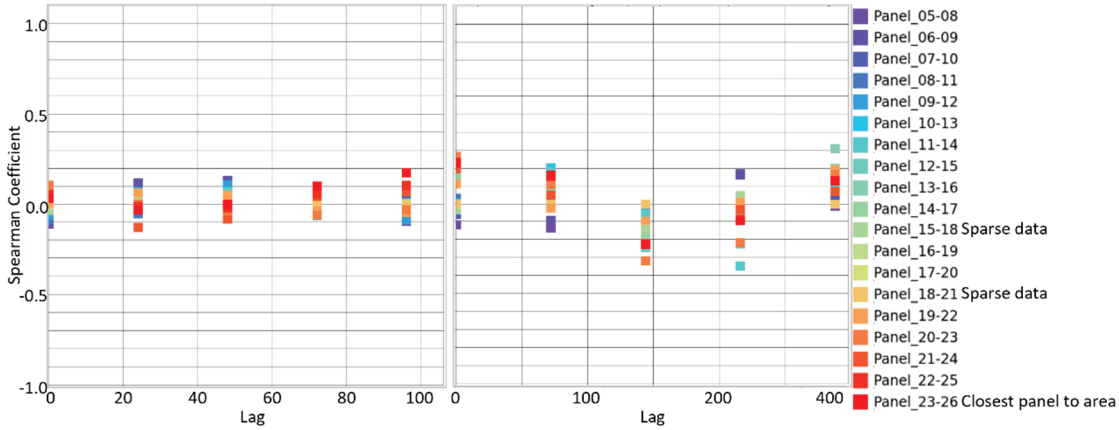

Figure 18 Spearman correlation coefficient calculated for the rate of change of the slopes of the cumulative potency in Area51, above the undercut, and the cumulative production blasting for time series sampled at equal time intervals Δt = 24h and 72h (left, right) and lag times $t_{Lag} = n \cdot \Delta t, n$ = 0, 1, 2, 3 and 4

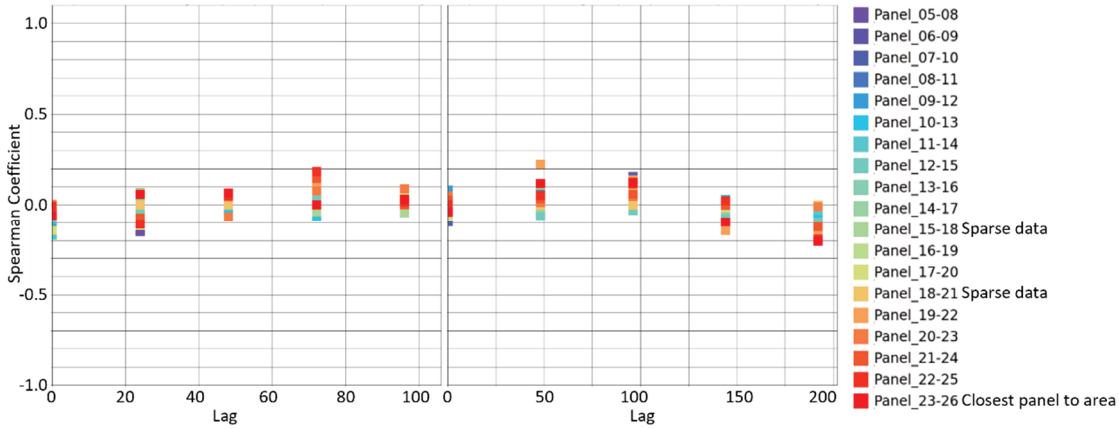

Figure 19 Spearman correlation coefficient calculated for the rate of change of the slopes of the cumulative potency in Area51, in and below the undercut, and the cumulative drawbell blasting for time series sampled at equal time intervals Δt = 24h and 48h (left, right) and lag times $t_{Lag} = n \cdot \Delta t, n$ = 0, 1, 2, 3 and 4

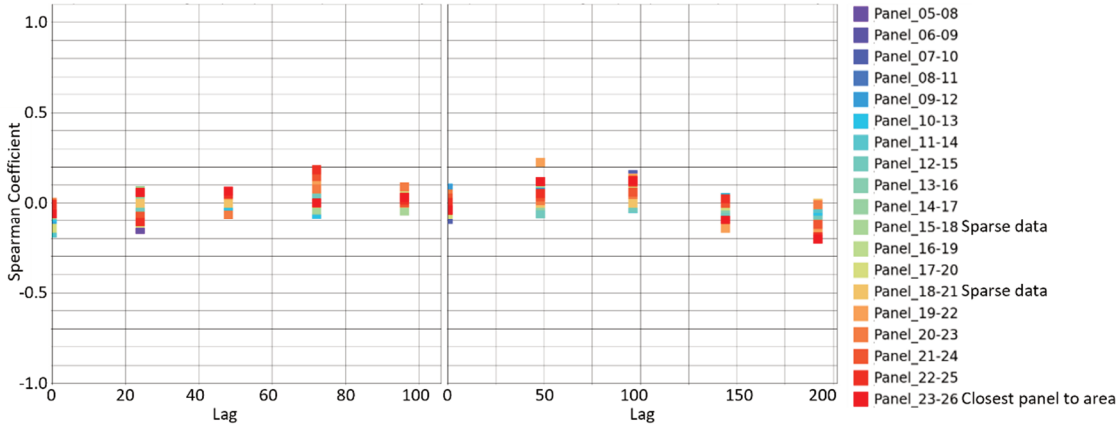

Figure 20 Spearman correlation coefficient calculated for the rate of change of the slopes of the cumulative potency in Area51, above the undercut, and the cumulative drawbell blasting for time series sampled at equal time intervals Δt = 24h and 48h (left, right) and lag times $t_{Lag} = n \cdot \Delta t, n$ = 0, 1, 2, 3 and 4

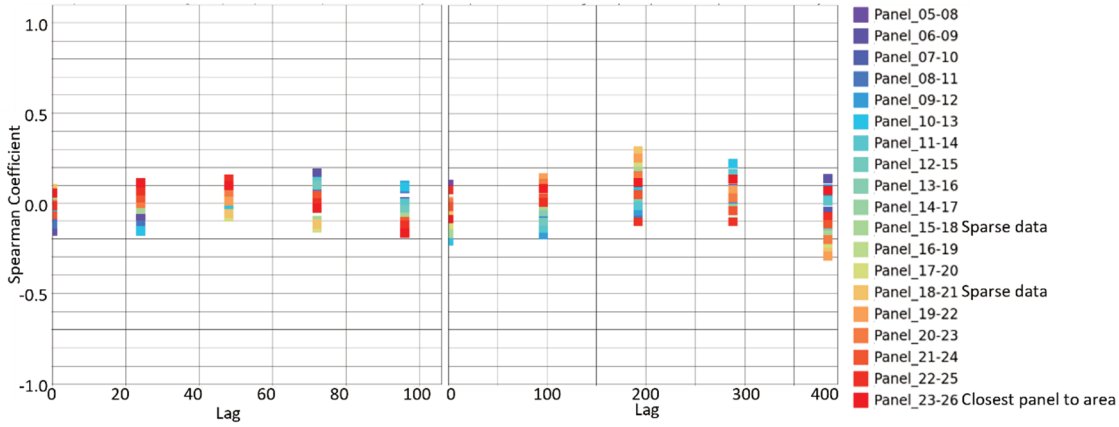

Figure 21 Spearman correlation coefficient calculated for the rate of change of the slopes of the cumulative potency in Area51, in and below the undercut, and the cumulative mucking for time series sampled at equal time intervals Δt = 24h and 96h (left, right) and lag times $t_{Lag} = n \cdot \Delta t, n$ = 0, 1, 2, 3 and 4

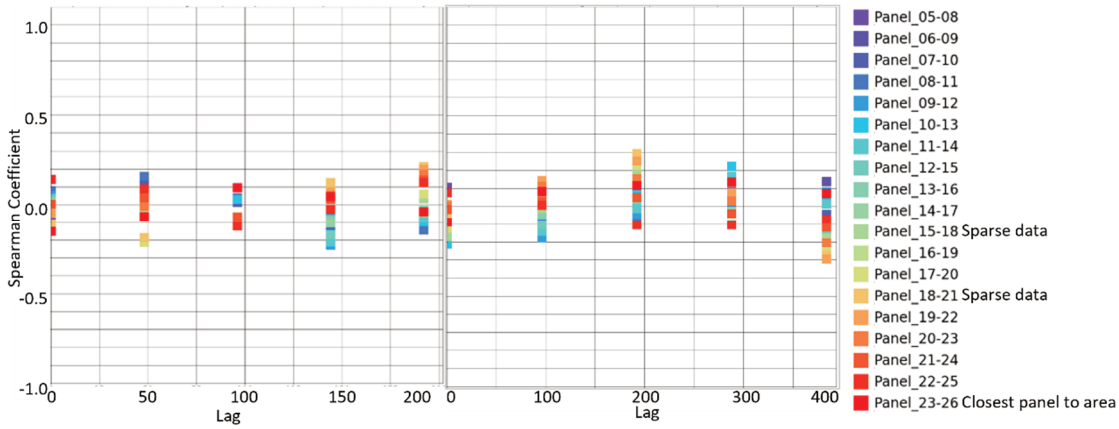

Figure 22 Spearman correlation coefficient calculated for the rate of change of the slopes of the cumulative potency in Area51, above the undercut, and the cumulative mucking for time series sampled at equal time intervals Δt = 48h and 96h (left, right) and lag times $t_{Lag} = n \cdot \Delta t, n$ = 0, 1, 2, 3 and 4

4.4 Summary

Tables 1 and 2 summarise the maximum r_S values and their associated sampling periods and lags of only the closest five or six panels. The correlation between bare cumulative quantities is as expected and carries no useful information beyond supporting the technique.

4.5 Comparative rate of seismic release

- The correlation for the rate of seismic release and the rate of production blasting in Area51 below the undercut is significantly higher than above the undercut. The time over which the change takes place and the lag between the production blasting rate and the seismic release rate below the undercut are half that above the undercut.
- In Area51 below and above the undercut, correlation of seismic release rate with drawbell blasting is very weak.
- The highest r_S (0.70) is associated with the slope of the cumulative mucking in the area, both under and above the undercut. However, note that this is for a change over four days, and a lag of eight days.

4.6 Comparative change of seismic release rate

The maximum correlation between change of seismic rate and the rates of change of all three production types are similar and strong for this dataset.

- The correlation for production blasting is like the rate of blasting, but the time components are significantly longer.
- For the drawbell blasts r_S is much larger than the coefficient for just the change in cumulative drawbell blasting.
- In the case of mucking, the correlation is significantly less than the for the slope of the mucking.

Table 1 Summary of results – Area51 below undercut

Variable	Maximum r_S (closer panels)	Sampling period Δt (h)	Lag t_{Lag} (h)
Cumulative potency and			
Cumulative production blasting	1.00	All	All
Cumulative drawbell blasting	1.00	All	All
Cumulative mucking	1.00	All	All
Rate of cumulative potency and			
Rate of cumulative production blasting	0.25	48	48
Rate of cumulative drawbell blasting	0.10	48	144
Rate of cumulative mucking	0.70	96	192
Change of rate of cumulative potency and			
Change of rate of cumulative production blasting	0.30	96	96
Change of rate of cumulative drawbell blasting	0.25	48	48
Change of rate of cumulative mucking	0.30	96	192

Table 2 Summary of results – Area51 above undercut

Variable	Maximum r_S (closer panels)	Sampling period Δt (h)	Lag t_{Lag} (h)
Cumulative potency and			
Production blasting	1.0	All	All
Drawbell blasting	1.0	All	All
Mucking	1.0	All	All
Rate of cumulative potency and			
Rate of cumulative production blasting	0.15	96	96
Rate of cumulative drawbell blasting	0.10	48	96
Rate of cumulative mucking	0.70	96	192
Change of rate of cumulative potency and			
Change of rate of cumulative production blasting	0.25	96	0
Change of rate of cumulative drawbell blasting	0.25	48	48
Change of rate of cumulative mucking	0.30	96	192

5 Conclusion

The question addressed in this paper is whether there are quantifiable correlations between production rates and seismic response. The strong correlation of the rate of seismic release with the rate of mucking over a relatively long period, and lagging the mucking significantly, suggest that the rate of mucking is a long-period driver of seismic release both above and below the undercut, a type of background driver. In and under the undercut, the larger correlation with the rate of production blasting, over a shorter period, with a shorter

lag, compared to the to the area above the undercut, supports the qualitative observation that the rate of production blasting is a more important driver of seismic release in and below the undercut than above it. This is consistent with the physical picture in this area, a stressed abutment with stress raisers like pillars and stiffness contrasts over contacts between different lithologies. The weak correlation with the rate of drawbell blasting compared to the rate of change of drawbell blasting implies that drawbell blasting is not a long-period, background driver. Rather, drawbell blasting provides short, sharp shocks to the rock mass system.

There are encouraging indications that the technique is useful: the correlation coefficients exhibit variation across variables, sampling periods and lag times. Further work will focus on increased spatial resolution and statistical significance, and on the effect of different stages in the life of a cave. The first will address the fact that we have considered not only several panels at once, but we have not distinguished between different sections of the panels (e.g. the northern, middle, and southern sections). The latter is required to provide an objective measure of confidence in the results. The third factor relates to the use of these correlations in managing cave performance.

Acknowledgement

The author acknowledges Lindsay Smith-Boughner, who suggested this approach.

References

Ben-Zion, Y, Lyakhovsky, V 2019, 'Representation of seismic sources sustaining changes of elastic moduli', *Geophysical Journal International*, vol. 217, pp. 135–139.

Clarke, GM, Cooke, D 1978, *A Basic Course in Statistics*, Edward Arnold, London.

Gibowicz, SJ & Kijko, A 1994, *An Introduction to Mining Seismology*, Academic Press, Cambridge.

Kaiser, P, Vasak, P, Suorineni, F & Thibodeau, D 2005, 'New dimensions in seismic data interpretation with 3-D virtual reality visualization for burst-prone mines', in Y Potvin & M. Hudyma (eds), *Proceedings of the Sixth International Symposium on Rockburst and Seismicity in Mines*, Australian Centre for Geomechanics, Perth, doi.org/10.36487/ACG_repo/574_0.3

McGarr, A 1976, 'Seismic moments and volume changes', *Journal of Geophysical Research*, vol. 81, pp. 1487–1494.